

# Effect of the Amine Functional Group on Corrosion Rate of Iron Coated with Films of Organofunctional Silanes

V. Subramanian and W.J. van Ooij\*

## ABSTRACT

Silane pretreatments were investigated as environmentally friendly replacements for the existing chromating processes. The objective was to compare the corrosion protection properties of various silanes. The corrosion inhibiting action of silane films on iron was examined in 3% sodium chloride (NaCl) solutions. Coatings made with two silanes, one with a functional group ( $\gamma$ -aminopropyltriethoxysilane [ $\gamma$ -APS]) and one without a functional group (bis-triethoxysilyl ethane, BTSE), were studied. Characterization of the silane films was performed by ellipsometry, reflection-absorption infrared spectroscopy (RA-IR), atom force microscopy (AFM), energy-dispersive x-ray analysis (EDX), and x-ray photoelectron spectroscopy (XPS). Corrosion rates were determined from polarization studies. It was found that  $\gamma$ -APS films had no effect on the corrosion rate of iron. However, BTSE films deposited from solutions of pH 4 to 6 reduced the corrosion rate by a factor of 15. The greater effect of a BTSE film was explained by formation of more stable Fe-O-Si bonds and the higher degree of cross-linking of the BTSE films compared to the  $\gamma$ -APS films.

**KEY WORDS:** atom force microscopy, electrochemical testing, ellipsometry, energy dispersive x-ray analysis, films and film formation, iron, polarization, reflection absorption-infrared spectroscopy, silanes, x-ray photoelectron spectroscopy

## INTRODUCTION

Organofunctional silane coupling agents have attracted the attention of researchers from academe and industry for more than three decades.<sup>1</sup> Silanes have the unique ability to form strong bonds both with the metal oxide and with the paint polymer. Oxane bonds (Me-O-Si) are formed through the silane end, and the functional groups can form chemical bonds with the paint polymer.<sup>1</sup> Formation of siloxane chains also can result in formation of interpenetrating polymer networks with the paint polymer at the interface.

In applying silanes to various substrates, the focus of research mainly has been to identify the appropriate silane and coating method, followed by optimization of the coating and curing conditions of the silane film. The organofunctional silane selected can have two or more hydrolyzable ester groups, can have some kind of unsaturation in its organic end so as to enhance polymerization, may or may be branched, and should have a functional group that stabilizes the silane-to-paint interface. Once the silane is selected, it is hydrolyzed. Then, the coating is made using one of various methods: solution dip,<sup>2</sup> vapor deposition,<sup>3</sup> plasma deposition,<sup>4</sup> electrodeposition,<sup>5</sup> spraying, brushing, or wiping. The films made can be cured to ensure polymerization and to remove water from the film. Various methods available for curing include heating, infrared curing, vacuum curing, and catalyst-assisted polymerization.

Submitted for publication October 1996; in revised form, April 1997.

\* Department of Material Science and Engineering, P.O. Box 210012, University of Cincinnati, Cincinnati, OH 45221-0012.

The process parameters for coating silanes on metals include the method of surface cleaning, choice of solvent,<sup>6-8</sup> the concentration of the silane, the pH of the solution,<sup>7,9,10-12</sup> the hydrolysis time and conditions,<sup>6,10</sup> the dipping time, and whether rinsing or blow drying is used to dry the film or whether it is dried in place. Curing conditions involve the selection of temperature and time in the case of curing by application of heat.<sup>7,9,13-14</sup>

The primary function of the functional group in an organofunctional silane is to improve the strength of the silane-paint polymer interface by formation of chemical bonds. However, these functional groups could have an effect on the corrosion protection. The literature confirms that adhesive failure at the metal-primer interface often is associated with the protonation of amino groups present. In the case of  $\gamma$ -aminopropyltriethoxysilane ( $\gamma$ -APS), excess protonation of the amino groups near the metal-silane interface was observed by x-ray photoelectron spectroscopy (XPS) for nine metals studied.<sup>15</sup> Failure analyses of adhesive joints showed the locus of failure was closer to the oxide-primer interface, where amine protonation was also higher.<sup>16-17</sup> The failure surfaces of aluminum-epoxy joints in which the aluminum substrates were pretreated with aliphatic amine curing agents showed a higher percentage of amine protonation than in the bulk of the cured adhesive.<sup>18</sup>

Organofunctional silanes can be used as coupling agents between metals and polymers.<sup>1</sup> Since corrosion protection of the base metal is one of the primary functions of a paint coating, corrosion protection properties are of extreme importance.

The corrosion behavior of iron coated with three types of silane films were investigated in the present work. The silane films were prepared by dipping. These silane films were characterized before and after corrosion testing, and a model for the corrosion process was proposed.

The effect of the amine functional group on corrosion protection properties of iron was investigated. The silanes selected for study were  $\gamma$ -APS ( $\text{H}_2\text{N}-\text{CH}_2-\text{CH}_2-\text{Si}(\text{OC}_2\text{H}_5)_3$ ) and 1,2-bis-(triethoxysilyl) ethane, or BTSE ( $[\text{H}_5\text{C}_2\text{O}]_3-\text{Si}-\text{CH}_2-\text{CH}_2-\text{Si}[\text{OC}_2\text{H}_5]_3$ ).  $\gamma$ -APS is the most widely studied functional silane.<sup>3</sup> BTSE is a nonfunctional silane often referred to as a cross-linker and is used to improve polymerization and silane film stability.<sup>19-20</sup> BTSE has shown good promise in improving the mechanical strength of adhesive joints.<sup>21</sup>

Polished pure iron substrates were coated with silanes; characterized by reflection-absorption infrared spectroscopy (RA-IR), atom force microscopy (AFM), energy-dispersive x-ray analysis (EDX), and XPS; and studied for corrosion protection using elec-

trochemical methods. Characterization by RA-IR, EDX, and XPS also was done on selected samples after corrosion testing. Results were discussed in terms of the film structure.

## EXPERIMENTAL

### Materials and Preparation of Silane Films

Iron foils of 99.5% purity were obtained commercially. These hard-tempered foils were polished with sandpaper, ground with diamond paste (1 micron) to obtain a mirror finish, rinsed with methanol, and blow dried with compressed air.

In the case of  $\gamma$ -APS, solutions were prepared by mixing 90% methanol, 4% silane, and 6% water, by volume. The pH of this solution was  $\approx 10.7$ . The solution pH was lowered by addition of acetic acid ( $\text{CH}_3\text{COOH}$ ). In the case of BTSE, the solution was made by mixing 4% silane, 0.4%  $\text{CH}_3\text{COOH}$ , 6% water, and 89.6% methanol by volume, in that order, to obtain a stable hydrolyzed silane solution. The pH of the solution was  $\approx 4.0$  in this case. Sodium hydroxide (NaOH) was used to increment the pH to 7, in steps. The solution started coagulating above neutral pH, resulting in a gradual increase of the solution pH without further addition of the base solution. The coatings were prepared at the selected pH values. The solution of the mixture was made by a method similar to  $\gamma$ -APS, and contained 4%  $\gamma$ -APS and 1% BTSE. The natural pH of this solution was close to 10.  $\text{CH}_3\text{COOH}$  was used to lower the pH, as in the case of  $\gamma$ -APS. All solutions were stirred for 60 min to hydrolyze the silanes to equilibrium.<sup>22</sup> The solution was considered to have stabilized once the rate of change of pH was  $< 0.01$  per min.

The polished iron foils were dipped in fresh silane solutions prepared as above for a duration of 100 s. The films obtained were first blow dried with air to obtain uniform thickness. Curing was done at 60°C for 1 h in air, with the aim of removing all solvents and to achieve a cross-linked silane film.

The conditions varied in this study were the types of silane used (functional silane, nonfunctional silane, or a mixture) and the pH of the coating solution (4 through 11).

### Film Characterization and Corrosion Testing

**Ellipsometry** — A Rudolph Research Model 436<sup>†</sup> ellipsometer was used in all measurements. In the calculation, the films were assumed to be isotropic, single-layered, and with a known refractive index. Thickness of all the silane films was calculated using McCrackin's program<sup>23</sup> and a refractive index of 1.424.<sup>21,24</sup> All thickness values were rounded to the nearest nanometer.

**RA-IR Analysis** — RA-IR spectra were collected using a BIO-RAD FTS-40<sup>†</sup> FT-IR spectrometer equipped with a BIO-RAD<sup>†</sup> variable angular reflec-

<sup>†</sup> Trade name.

**TABLE 1**  
*Thickness of Silane Films Formed on Iron Substrates<sup>(A)</sup>*

pH of the Coating Solution	Thickness of Film ( $\gamma$ -APS) (nm)	Thickness of Film ( $\gamma$ -APS + BTSE) (nm)	Thickness of Film (BTSE) (nm)
4	74	96	91
5	77	92	86
6	82	98	86
7	86	95	91
8	82	100	90
9	85	91	82
10	88	88	86
11	80	90	81

<sup>(A)</sup> Films formed by solution dipping for 100 s and curing at 60°C for 60 min in air; measured by ellipsometry; values are averages of three measurements.

tance attachment at an incidence angle of 75°. Dry air was used for purging. The interferograms were acquired for 128 scans using 4 /cm resolution. Each spectrum was obtained by subtracting a background spectrum obtained for the pure iron substrate before depositing the silane coating.

**XPS Analyses** — XPS analysis was carried out using a Perkin-Elmer 5300<sup>†</sup> XPS system. Magnesium K $\alpha$  radiation of 300 W was used. Pass energies for the survey and narrow scans were 44.7 eV and 17.9 eV, respectively. To correct for sample charging, all binding energies were referenced to the aliphatic C1s peak at 284.6 eV. A takeoff angle of 75° between the sample surface and the analyzer entrance was used for all samples analyzed. Quantification was performed by determining peak areas assuming a Shirley background model. Details about various curve fitting processes used to aid interpretation of XPS spectra have been reported previously.<sup>25</sup> As the sampling depth in XPS was limited to  $\approx$  60 Å, these measurements were useful only for characterization of the outermost surface of the silane films. As these films had a thickness in the range of 100 Å to 1,000 Å before corrosion testing, no information about the metal-silane interface could be obtained.

**EDX Characterization** — All EDX measurements were performed on a Cambridge 90B<sup>†</sup> SEM equipped with Princeton Gamma Tech<sup>†</sup> EDS system. An acceleration voltage of 15 kV was used to probe well into the substrate through the silane layer.

**AFM Characterization** — AFM images of polished pure iron substrates with and without silane films were obtained on a Burleigh Instruments ARIS-3500 Personal AFM<sup>†</sup> system. Samples were analyzed at ambient conditions. The AFM equipment was operated in the contact mode. During imaging, the micromachined silicon cantilever was in contact with the surface under a reference force of  $\sim$  2.11 N. The topography of the surface was a measurement of the adjustment in the vertical direction necessary to keep the reference force constant.

**Corrosion Measurements** — The corrosion rate for the coated metals was determined by conducting forward polarization tests, using a Gamry Instruments CMS 100<sup>†</sup> corrosion measurement system. The analysis was performed using the software provided with the equipment. The voltage range was typically  $\pm$  200 mV, and the scan rate was 1 mV/s. Varying the scan rates in the case of Tafel testing did not change the results, even when the scan rates were reduced to 0.125 mV/s, which equaled the polarization resistance testing rates. Aerated 3% sodium chloride (NaCl) solutions were used as the electrolyte. The steady-state corrosion current ( $i_{\text{corr}}$ ) obtained from the Tafel plots was converted to corrosion rates in mpy (millimeters per year).<sup>26-27</sup> All electrochemical tests for the coated metals were repeated at least 10 times. Figures show the average values and the standard deviation in each case.

## RESULTS AND DISCUSSION

### Film Thickness

Table 1 shows the results of ellipsometry thickness measurements, giving the thickness of the silane film as a function of pH of the solution. In each case, at least three samples were characterized, and the average values are listed. Multiple factors affect the thickness, including the condensation polymerization in the solution, the surface potential variation of the substrate with the pH of the solution it was in contact with, and the mode of attachment of the silane. However, these factors did not result in any appreciable variation in the thickness of the three types of silane films studied.

### Corrosion Rates

Corrosion rates obtained are summarized in Figure 1. In the case of  $\gamma$ -APS and in the case of the silane mixture, the effect of pH was not appreciable. However, much lower corrosion rates were obtained for iron substrates coated with BTSE from

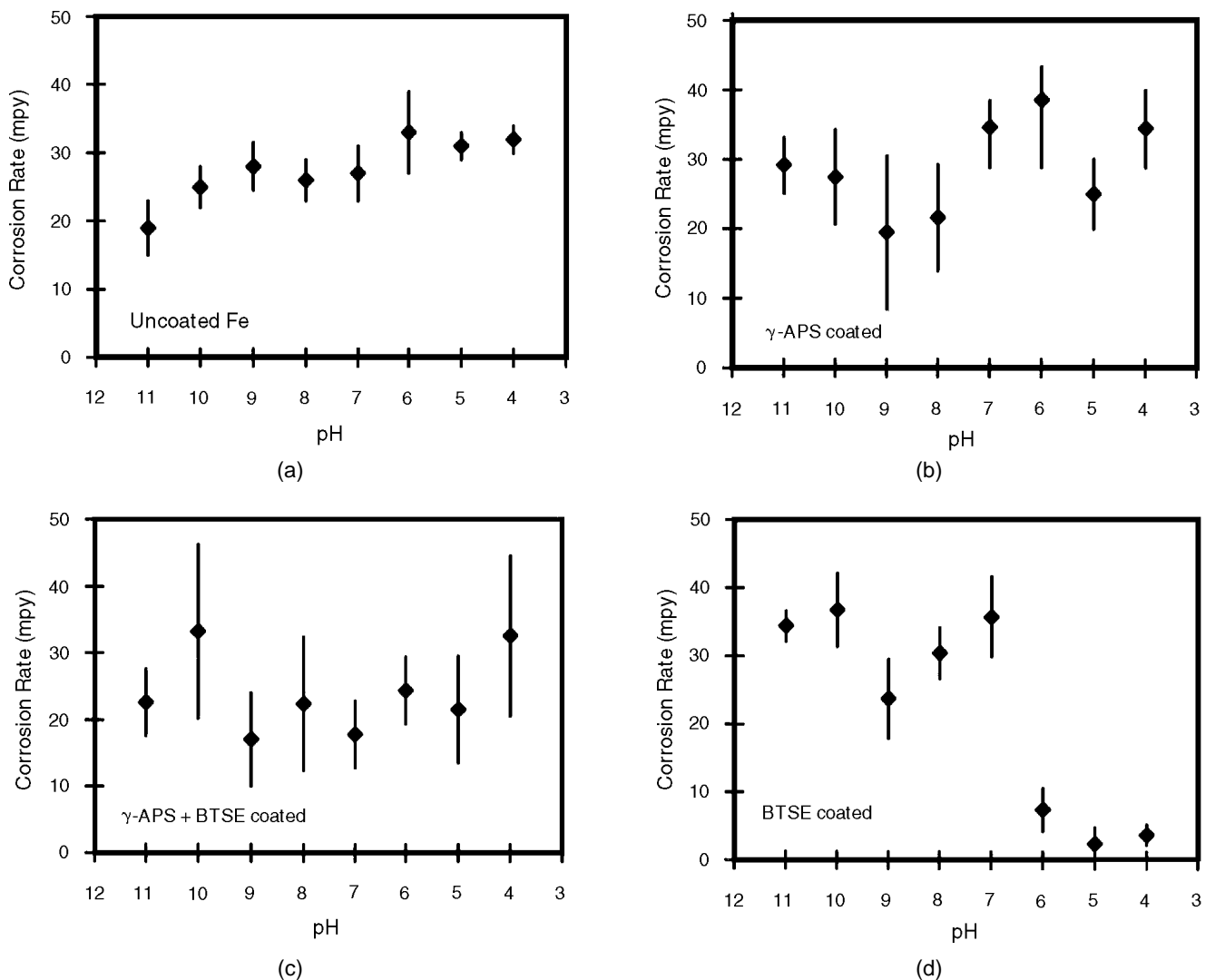


**FIGURE 1.** Corrosion rates as a function of pH for: (a) uncoated iron, (b)  $\gamma$ -APS-coated iron, (c)  $\gamma$ -APS + BTSE-coated iron, and (d) BTSE-coated iron. Dipping time was 100 s, and concentration of the silanes in solution was 4 vol% in the case of single silanes and 4 vol% plus 1 vol% in the case of the mixture. Curing was at 60°C in air for 1 h.

low-pH solutions. Figure 1 shows clearly the difference between corrosion rates of iron coated with BTSE films formed from low pH values and all the other films studied. These figures also show that the presence of  $\gamma$ -APS in the film had hardly any effect on corrosion rates. However, pure BTSE films formed from low pH values were effective in reducing corrosion rates markedly. Figure 2 shows a comparison between typical polarization curves for iron coated with  $\gamma$ -APS from a solution of pH 11 and iron coated with BTSE from a solution of pH 5.

In the case of BTSE, it already has been noted that the solution was unstable at pH > 7. EDX analysis of silane films formed from basic pH levels showed the presence of sodium, and the RA-IR analysis showed the presence of acetate ions.

Visual examination confirmed that corrosion in each case was uniform on a macroscale. The uniformity of the corrosive attack on a microscale was confirmed by AFM.

#### RA-IR characterization

RA-IR characterization was done on samples coated from the silane solutions before and after the corrosion tests. Typical spectra obtained with films coated from solutions of basic and acidic pH values are shown in Figures 3 through 5 for the three silane coatings studied. Table 2 shows the peak assignments used to characterize the films.<sup>28</sup>

In Figure 3, the presence of a condensed film of  $\gamma$ -APS was asserted by the presence of strong peaks at 1,150  $\text{cm}^{-1}$  to 1,050  $\text{cm}^{-1}$  (Si-O-Si peaks), indicating the formation of a siloxane film at all pH values

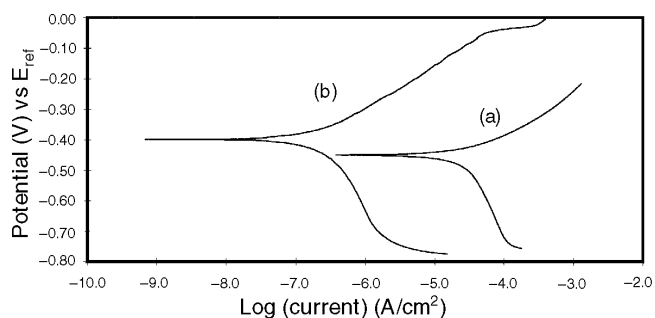


**FIGURE 2.** Comparison of polarization curves obtained in 3% NaCl solutions for: (a) iron coated with  $\gamma$ -APS film from pH = 11 and (b) iron coated with BTSE film from pH = 5.

studied. Similar peaks established the formation of siloxane films for the cases of the mixture (Figure 4) and BTSE (Figure 5). These complemented the ellipsometry measurements, conforming the presence of siloxane films in all cases studied.

Various cross-linking agents, such as BTSE, could be added to the silane solution in an attempt to improve stability of the silane film.<sup>29</sup> Hence, silane films also were formed from solution containing both  $\gamma$ -APS and BTSE. The IR spectra of such films are shown in Figure 4. The stronger peaks at 1,150  $\text{cm}^{-1}$  to 1,050  $\text{cm}^{-1}$  proved BTSE was indeed incorporated in the film formed. The process of corrosion resulted in weakening of the amine peaks in the range from 1,550  $\text{cm}^{-1}$  to 1,600  $\text{cm}^{-1}$ , indicating the BTSE molecules were retained in the film to a higher degree than the  $\gamma$ -APS molecules during the corrosion process.

The IR spectra of  $\gamma$ -APS (Figure 3) showed a single broad peak in the 1,200  $\text{cm}^{-1}$  to 1,100  $\text{cm}^{-1}$  region. The BTSE films (Figure 5), on the other hand, showed two strong peaks in the same region. The second peak at 1,160  $\text{cm}^{-1}$  resulted from the Si-O-C vibrations. A broad peak at 960  $\text{cm}^{-1}$  confirmed the presence of unhydrolyzed Si-O-C<sub>2</sub>H<sub>5</sub> groups. This showed that, in the case of BTSE, the hydrolysis of Si-O-C<sub>2</sub>H<sub>5</sub> ester groups was incomplete, in agreement with the literature.<sup>22</sup> The peak at 960  $\text{cm}^{-1}$  was stronger at pH 5 than at pH 11. This was attributed to the

relatively lower hydrolysis rate for BTSE at pH 5 than at pH 11.<sup>22</sup>

In the case of pure BTSE films formed from basic pH values and all films containing  $\gamma$ -APS, a sharp peak around 1,600  $\text{cm}^{-1}$  and a smaller peak around 1,400  $\text{cm}^{-1}$  were found. Together, these two peaks indicated the presence of carboxylic acid salts.<sup>30</sup> The amine peak, which also fell in the same range of wavenumbers (1,600  $\text{cm}^{-1}$  to 1,550  $\text{cm}^{-1}$ )<sup>30</sup> was masked by the stronger acid peak. Both acid peaks were absent in the case of BTSE films formed from solutions with pH values < 6. It was inferred that the BTSE film formed from low pH values did not contain any incorporated acid salts, while all other films had acetate ions incorporated.

Considering the  $\gamma$ -APS films after corrosion testing (Figure 3), the acid peak (1,600  $\text{cm}^{-1}$  and 1,400  $\text{cm}^{-1}$ ) intensities decreased, while the Si-O-Si peak intensity was retained. The amine peaks also fell in the 1,550  $\text{cm}^{-1}$  to 1,600  $\text{cm}^{-1}$  range. Thus, the acid groups present in the film partly were washed away during the corrosion process. Another possibility was that these acid groups were converted to various salts, which were soluble in the corroding medium. The evolution of the Si-OH peak at 910  $\text{cm}^{-1}$  indicated partial hydrolysis of the siloxane film or the Fe-O-Si oxane bonds occurred during the corrosion process.

CH<sub>3</sub>COOH was used both to hydrolyze BTSE and to adjust the pH of the silane solution. The peak at 1,740  $\text{cm}^{-1}$ , as observed in many of the films studied, was assigned to the carbonyl group stretch vibrations of esters formed by the reaction of these acid molecules with the alcohol in the system.

### Characterization of Silane Films by AFM

Selected silane films also were analyzed using AFM. Figure 6(a) shows the surface scan of a blank Fe coupon. Figure 6 also shows  $\gamma$ -APS films formed at pH 11 (Figures 6[b] and [c]) and BTSE films formed at pH 5 (Figures 6[d] and [e]) scanned before and after corrosion testing. These figures show the silane films formed under the conditions studied were con-

**TABLE 2**  
RA-IR Peak Assignments<sup>25</sup>

Wavenumber ( $\text{cm}^{-1}$ )	Assignments
1,750 to 1,740	C=O carbonyl stretch
1,600 to 1,575	NH <sub>2</sub> group deformation. Shifts to higher wavenumbers if protonated.
1,620 to 1,580	COO <sup>-</sup> group of carboxylic acids
1,480 to 1,470	Aliphatic CH <sub>2</sub> symmetric scissor
1,420 to 1,400	Salts of carboxylic acids
1,340 to 1,330	Aliphatic C-H bending
1,180 to 1,160	Si-O-C <sub>2</sub> H <sub>5</sub> group of unhydrolyzed silanes
1,150 to 1,050	Si-O-Si bonds of siloxanes — double peak seen from long chain polymers of Si-O-Si form <sup>28</sup>
970 to 950	Si-O-C <sub>2</sub> H <sub>5</sub> group of unhydrolyzed silanes
920 to 900	Si-O-H group of hydrolyzed silanes

tinuous. There was a marked difference in the surface smoothness of the  $\gamma$ -APS and BTSE films, the latter ones being smoother than the former. The better wettability of the substrate by the BTSE was evident from these figures. Another noticeable aspect was that the corrosion testing resulted in a rougher film in both cases studied. It could be concluded that, for both these films, corrosion was uniform on a microscopic scale, as no evidence of film rupture was seen. Macroscopic uniformity was confirmed by visual examination.

### Characterization of Silane Films by XPS and EDX

To understand the specific chemical reactions occurring in the silane film during the corrosion process, selected samples were subjected to XPS analysis before and after the corrosion process. Two samples were selected:  $\gamma$ -APS coated from basic conditions (pH = 11), and BTSE coated from acidic conditions (pH = 5). The bulk concentration of specific atoms and the percentage of these atoms at specific binding energies were combined to obtain the surface percentage of each bond on the sample surface analyzed. EDX was used to estimate the bulk concentration of Si and Cl on the surface, before and after corrosion. Results are tabulated in Tables 3 through 5.

The XPS spectra of  $\gamma$ -APS and BTSE films showed the emergence of iron and chlorine peaks after corrosion. This apparently indicated the metal diffused out through the film while the chloride ions ( $\text{Cl}^-$ ) diffused inward. Concentrations of the metal were comparable in the two films. The  $\text{Cl}^-$  concentration, however, was higher (2.9%) in the case of the  $\gamma$ -APS film compared to the BTSE film (0.7%). This indicated that, even though both films permitted diffusion, the kinetics of  $\text{Cl}^-$  diffusion were different. A reduction in the concentration of Si was noticed after corrosion in both silane films. However, the drop was noticeable in the case of the  $\gamma$ -APS film (11.5% to 8.0%), while the BTSE film did not show any change (14.7% to 14.0%).

EDX results confirmed these results (Table 5). In the case of  $\gamma$ -APS film, the amount of Si decreased almost 90% during corrosion. In comparison, the amount of Si decreased by only  $\sim 10\%$  in the BTSE film. Thus, the BTSE film was much more stable, even under the application of a driving force, which in this case was the applied voltage. The decrease in Si concentration also could be looked upon as the reduction in the thickness of the silane film during the corrosion process. It has been demonstrated that the Si/Fe ratio for silane films varies directly with the thickness in the range from 0 nm to 500 nm.<sup>21</sup> The  $\gamma$ -APS film, thus, tended to undergo dissolution to a much higher degree than the BTSE film during corrosion testing.

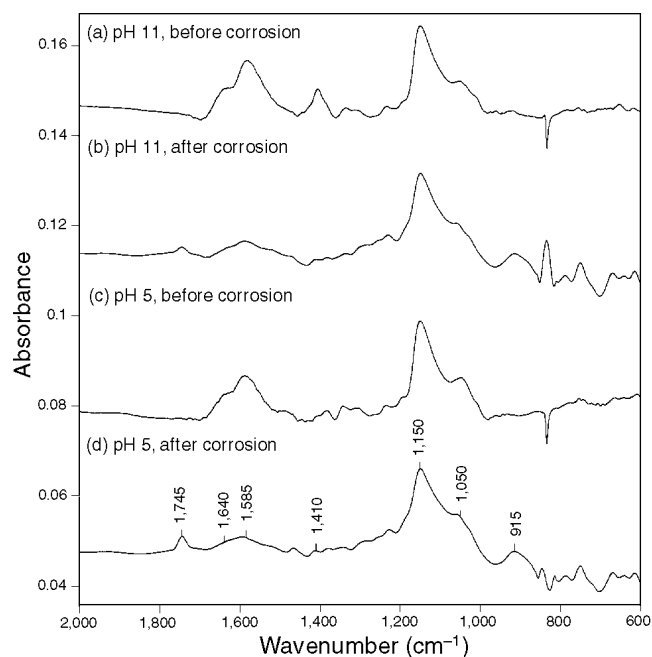


**FIGURE 3.** RA-IR spectra of iron samples coated with  $\gamma$ -APS films from: (a) pH = 11 before corrosion testing, (b) pH = 11 after corrosion testing, (c) pH = 5 before corrosion testing, and (d) pH = 5 after corrosion testing. Concentration of  $\gamma$ -APS in solution was 4 vol%, and dipping time was 100 s. Curing was at 60°C in air for 1 h.

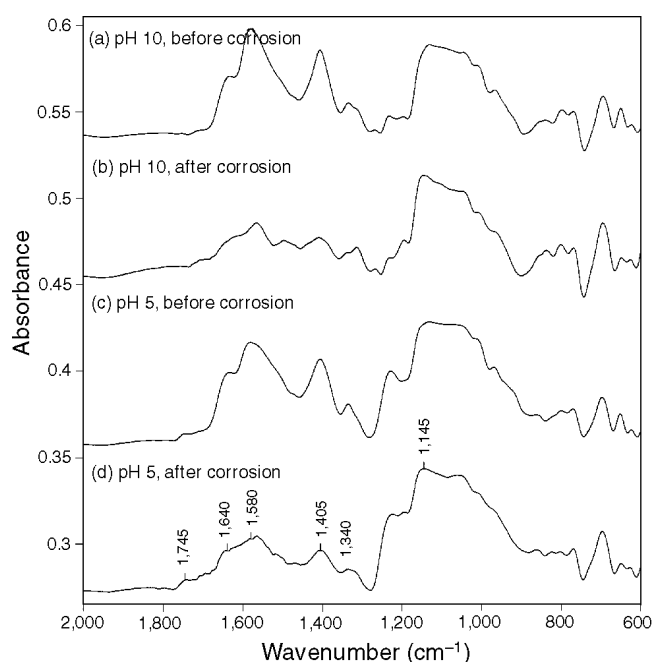


**FIGURE 4.** RA-IR spectra of iron samples coated with  $\gamma$ -APS + BTSE films from: (a) pH = 10 before corrosion testing, (b) pH = 10 after corrosion testing, (c) pH = 5 before corrosion testing, and (d) pH = 5 after corrosion testing. Dipping time was 100 s, and concentration of the silanes in solution was 4 vol% plus 1 vol%. Curing was at 60°C in air for 1 h.

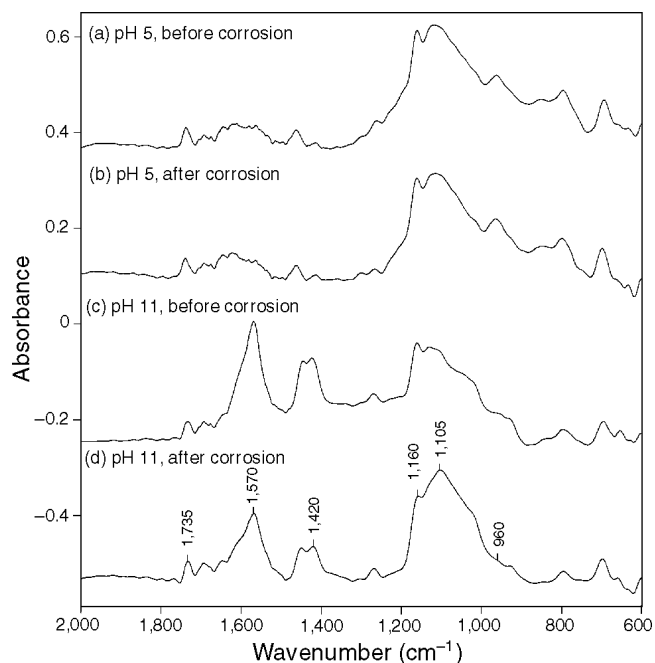


**FIGURE 5.** RA-IR spectra of iron samples coated with BTSE films from: (a) pH = 5 before corrosion testing, (b) pH = 5 after corrosion testing, (c) pH = 11 before corrosion testing, and (d) pH = 11 after corrosion testing. Concentration of BTSE in solution was 4 vol%, and dipping time was 100 s. Curing was at 60°C in air for 1 h.

The amount of Cl<sup>-</sup> also provided useful information. The Cl<sup>-</sup> concentration in the  $\gamma$ -APS film after corrosion was 0.7%. The BTSE films showed a lower Cl<sup>-</sup> ratio of 0.5%. Once, the thickness of these films was taken into account, the Cl<sup>-</sup> concentration in the  $\gamma$ -APS film was orders of magnitude higher than that in the BTSE film. Thus, the EDX and XPS measurements complimented each other, and together confirmed that the Cl<sup>-</sup> ions were not adhered just on the silane film surface, but penetrated deep into the film, with the amount absorbed by the film being considerably higher in the case of  $\gamma$ -APS films.

The oxygen 1s spectra are shown in Figure 7. Si-O-Si bonds corresponded to the stronger component around 532 eV.<sup>32</sup> The lower binding energy component indicated the presence of oxygen as iron oxides. This lower binding energy peak had a lower intensity (12%) in the case of BTSE films compared to  $\gamma$ -APS films (20%). Since both silane films showed comparable amounts of iron in the XPS analyses (Table 3), it was inferred that oxidation of the metal was a faster process in the  $\gamma$ -APS film. The corrosion rates for iron coated with BTSE also were found to be an order of magnitude lower than the  $\gamma$ -APS-coated iron.

Considering the surface composition of various oxygen bonds (Table 4), a pattern was noticed. In the case of BTSE films, the Si-O bond percentage was unchanged. The drop in the C-O bond percentage (4.0%) was matched with an increase in the Me-O

bond percentage (4.4%). A lowering in the surface composition of various bonds containing carbon also was evident. These observations, when combined, suggested the Si-OC<sub>2</sub>H<sub>5</sub> bonds in BTSE were replaced with Si-O-Me bonds during the corrosion process, along with the removal of ethanol molecules from the film surface. The Si-OR bonds hydrolyzed, and the silanol groups bonded Fe<sup>2+</sup> ions. Such a process would reduce the metal diffusion outward. It was found that the surface concentration of the metal was identical in both films (1.1% and 1.0%), even though the corrosion rates were markedly different. Corrosion, in the case of a silane-coated metal, thus could be considered as the outward diffusion of the metal through the film. Hence, the process of diffusion was reduced considerably by bonding the diffusing metal in the film by silanol groups formed in the corrosion process, as observed in the case of the BTSE film.

No such pattern was observed in the case of the  $\gamma$ -APS film. However, a general increase in the surface composition of all carbon-containing bonds and a reduction in the N, O, and Si contents were noticed, pointing toward a possible rearrangement of the silane molecules during the corrosion process. The corrosion process resulted in an increase in the surface concentration of O-Me bonds, but this was attributed to the oxide corrosion products that accumulated in the silane film during the corrosion process. The surface concentration of the C-N/C-O bonds in the  $\gamma$ -APS film did not change during the corrosion process. This aspect stood out in comparison with the BTSE film, where the reduction in the C-O bond concentration was matched with an increase in the Si-O-C bond concentration.

Corrosion, thus, involved the diffusion of Fe outward through the silane film. The anodically dissolved Fe ions hydrolyzed the water in the film under formation of Fe(OH)<sup>+</sup>, Fe(OH)<sub>2</sub>, and H<sub>3</sub>O<sup>+</sup> ions. The dissolving ferrous ions thus lowered the pH of the silane film. The lowering of the pH of the silane film resulted in protonation of the amino groups (Figure 8) in the case of a  $\gamma$ -APS film.

The nitrogen peaks obtained from the  $\gamma$ -APS films before and after corrosion are shown in Figure 8. The main N1s peak around 399.0 eV was attributed the -NH<sub>2</sub> groups present in the film. The second peak at around 400.6 indicated many of these amino groups were in the protonated state of -NH<sub>3</sub><sup>+</sup>.<sup>15</sup> Quantitative analyses of these peaks showed the percentage protonation of the amino groups was 42% after corrosion testing (Figure 8[b]), as opposed to 15%, measured before corrosion (Figure 8[a]). This clearly indicated the amino groups were indeed protonated during the corrosion process, which was attributed to reduction of the pH as a result of the anodic dissolution of the metal. The higher signal-to-noise ratio in the case of Figure 8(b) probably was a

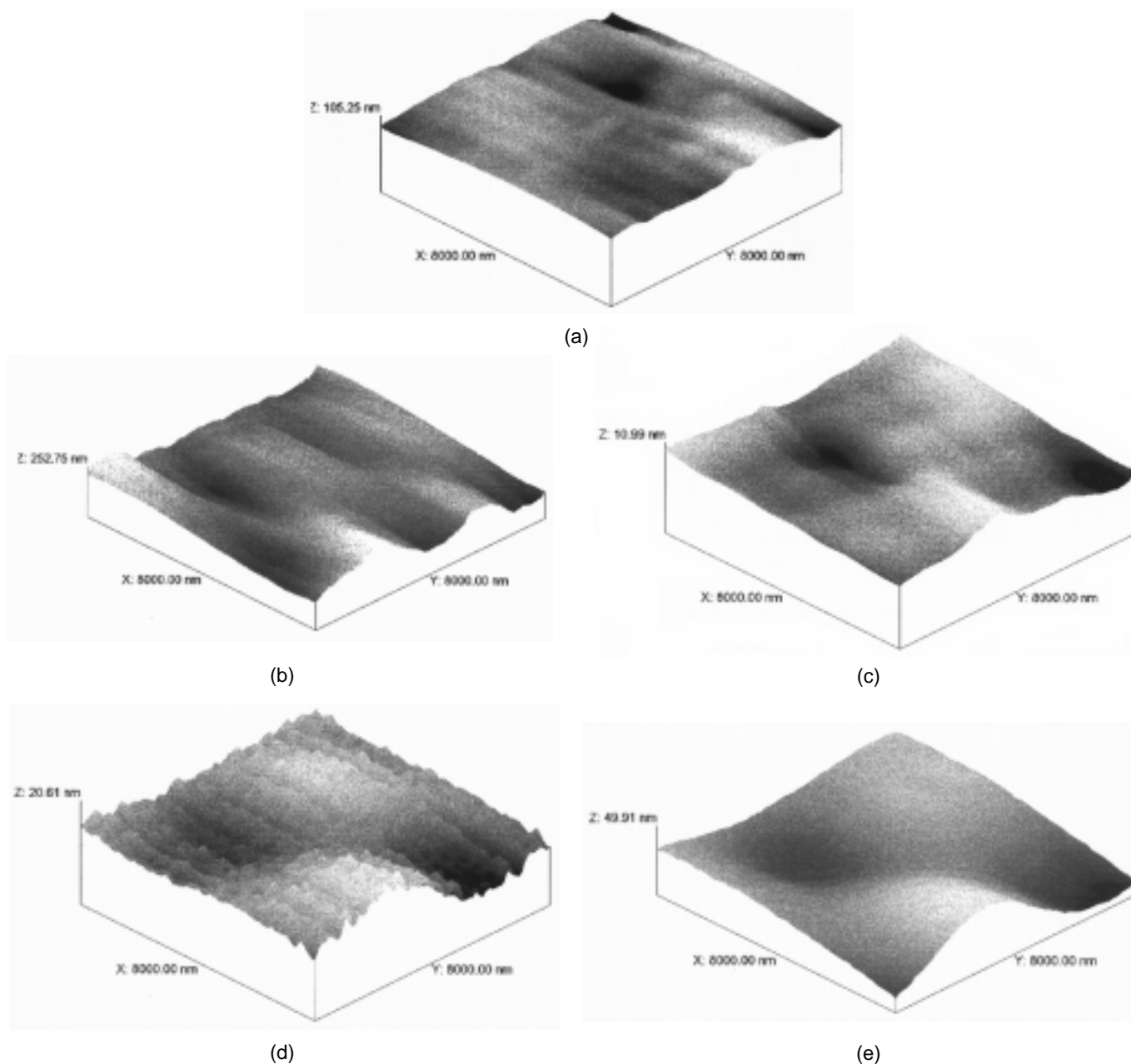


**FIGURE 6.** AFM three-dimensional image of: (a) polished pure iron substrate, (b) coated with  $\gamma$ -APS film scanned before, (c) scanned after corrosion (solution concentration was 3 vol%, dipping time was 100 s, and pH of the applied solution was 11); (d) coated with BTSE film and scanned before; and (e) scanned after corrosion (solution concentration was 3 vol%, dipping time was 100 s, and pH of the applied solution was 5).

result of the lower thickness and higher roughness of the  $\gamma$ -APS film after corrosion.

The positive point charges, created by the protonation of the amino groups, accelerated the migration of  $\text{Cl}^-$  ions toward the metal surface. A difference was indeed noted in the amount of chlorine present in the two types of silane films. The XPS results showed the  $\gamma$ -APS films had a higher percentage of chlorine, almost 3%, compared to the BTSE films, which contained only  $\sim 0.7\%$  chlorine. The

difference also was clear in the EDX results.  $\gamma$ -APS films showed a Cl/Si ratio of 0.9, while the BTSE films showed 0.07.

#### Model for the Corrosion Process

A model for the corrosion process of silane-coated iron and the positive effect of the BTSE films could be put forward based upon these results.

Films of  $\gamma$ -APS on iron and the mixture of  $\gamma$ -APS and BTSE were found to have virtually no effect on

**TABLE 3**  
XPS Surface Composition (%) of Iron Samples Coated with Silane

Coating Conditions	C	O	Si	N	Fe	Cl
$\gamma$ -APS, pH = 11, before corrosion	48.4	30.9	11.5	9.2	—	—
$\gamma$ -APS, pH = 11, after corrosion	54.7	25.8	8.0	7.5	1.1	2.9
BTSE, pH = 5, before corrosion	51.7	33.6	14.7	—	—	—
BTSE, pH = 5, after corrosion	46.3	38.0	14.0	1.0	0.7	—

**TABLE 4**  
XPS Binding Energy Assignments

Sample	Peak	State	Before Corrosion			After Corrosion		
			Binding Energy (eV)	$\theta = 75^\circ$ (%)	Surface (%)	Binding Energy (eV)	$\theta = 75^\circ$ (%)	Surface (%)
$\gamma$ -APS	C1s 1	C-C/C-H	284.6	67.3	32.6	284.6	70.4	38.5
	C1s 2	C-N/C-O	285.8	25.7	12.4	286.1	23.1	12.6
	C1s 3	C=O	287.6	7.0	3.4	287.9	6.5	3.6
	N1s 1	-NH <sub>2</sub>	399.0	84.8	7.8	399.0	58.1	4.4
	N1s 2	-NH <sub>3</sub> <sup>+</sup>	400.6	15.2	1.4	400.6	41.9	3.1
	Si2p	O-Si-O	102.4	1000	11.5	102.0	100	8.0
	O1s 1	O-Si	532.0	100	30.9	531.9	79.9	20.6
	O1s 2	O-Me				529.9	20.1	5.2
	Fe							1.1
	Cl							2.9
	Total							100.0
	BTSE	C1s 1	C-C/C-H	284.6	61.6	31.8	284.6	65.7
C1s 2		C-O	286.5	38.4	19.9	286.5	34.3	15.9
Si2p		Si-O	102.4	1000	14.7	102.3	100	14.0
O1s 1		O-Si	532.0	100	33.6	532.2	88.5	33.6
O1s 2		O-Me				529.8	11.5	4.4
Fe								1.0
Cl								0.7
Total								100.0

**TABLE 5**  
Surface Composition (%) of Samples Measured Before and After Corrosion Using EDX at 15-kV Acceleration Voltage

Coating Conditions	Fe	Si	Cl	Cl/Si
Uncoated, before corrosion	100.0	—	—	—
Uncoated, after corrosion	100.0	—	—	—
$\gamma$ -APS, pH = 11, before corrosion	92.0	8.0	—	0.0
$\gamma$ -APS, pH = 11, after corrosion	98.5	0.8	0.7	0.88
BTSE, pH = 5, before corrosion	91.7	8.3	—	0.0
BTSE, pH = 5, after corrosion	92.0	7.5	0.5	0.07

the corrosion rate of Fe in aerated NaCl solutions, even at thicknesses close to 0.1  $\mu\text{m}$ . Apparently, such films allowed diffusion of electrolyte into and out of the film without any hindrance, despite the presence of cross-links in the film as a result of the heat treatment. Also, the rate of dissolution of the iron substrate practically was unaffected; hence, the iron surface was not passivated by the silane film. It has been demonstrated recently that  $\gamma$ -APS has two modes of adsorption on an iron surface, namely, adsorption via the amino groups and adsorption via

the silanol groups. This conclusion was based on analysis of the silane films by time-of-flight SIMS.<sup>2,32</sup> The ratio of the two modes was on the order of 50/50. The silanol groups could be expected to form covalent Fe-O-Si bonds with the iron oxide surface upon heating and, thus, become more resistant to hydrolysis.<sup>2</sup> However, the primary amino groups could interact only with the iron oxide by forming hydrogen bonds. Such bonds are sensitive to hydrolysis and would lead to an accumulation of water at the interface, even if the film was cross-linked by a heat treatment following deposition.<sup>2</sup> Thus, when a silane film coated on steel is tested in a polarization experiment, it can be expected that the amino groups will not hinder the rate of anodic dissolution of the iron substrate.

Another factor to be considered is the concentration of electrolyte in the silane film. The  $\gamma$ -APS silane films can be expected to have relatively large amounts of water as a result of hydrogen bonding interaction between water molecules and the free amino groups. The free silanol groups, if still present, also will attract water molecules. The anodically dis-

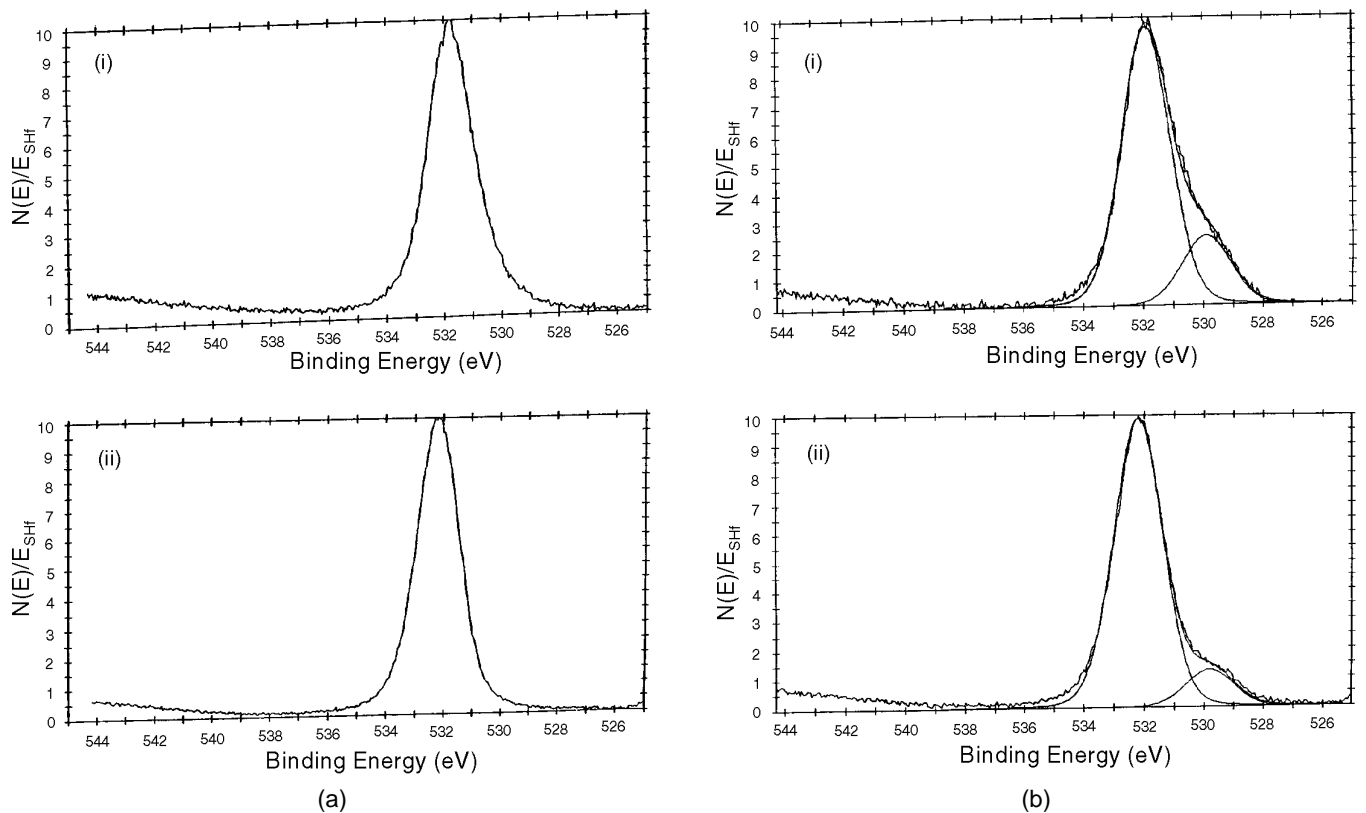


**FIGURE 7.** Deconvoluted O1s peaks for: (a)  $\gamma$ -APS and (b) BTSE films on iron: (a) before corrosion and (b) after corrosion. Concentration of the silane was 4 vol%, and dipping time was 100 s. Curing was at 60°C in air for 1 h.

solved Fe ions hydrolyze the water in the film under formation of  $\text{Fe}(\text{OH})^+$ ,  $\text{Fe}(\text{OH})_2$ , and  $\text{H}_3\text{O}^+$  ions. The pH thus drops and the  $\text{H}_3\text{O}^+$  ions will protonate the free amino groups in the films, as has been observed by RA-IR and XPS. In this mechanism, the anodically formed positive charges are retained by the silane film and cannot diffuse away from the surface. As a result, negative ions from the electrolyte will be attracted to the positive charges in the film and will diffuse inward. Thus, the  $\gamma$ -APS film will contain a high concentration of  $\text{Cl}^-$  ions. These silane films also contain acetate anions that contribute to the charge transport through the film during corrosion. The overall result of these processes is that the film will have a high conductivity and the iron substrate can corrode freely, despite the presence of some covalent Fe-O-Si bonds at the surface. The  $\gamma$ -APS film, thus acts as a semipermeable membrane toward the diffusing species, undergoing partial dissolution during the corrosion process.

The films formed from mixtures of  $\gamma$ -APS and BTSE exhibited the same behavior as those of the pure  $\gamma$ -APS, regardless of the pH from which the films were prepared. The conclusion that could be drawn from this observation was that the number of covalent Fe-O-Si bonds and the electrolyte concentrations of such films apparently were not noticeably

changed if 20% of the silane molecules present in the silane solution were replaced with BTSE. Such films have a higher degree of cross-linking and solvent resistance.<sup>2</sup> However, the results obtained in this work indicated that the number of amino groups adsorbed on the metal surface from the mixed solution was not significantly different. Amine groups, if present in the silane, tend to compete with the Si-OH groups to form bonds with the hydroxyl groups on the substrate, during the coating stage. The bonds formed in this case were hydrogen bonds, which were weak relative to the strong oxane bonds formed by the silanol group, and were easily broken during the corrosion process.

In the case of films formed from BTSE alone, the situation was drastically different. Since BTSE is a bifunctional silane, the concentration of the silanol groups in solutions of this silane molecule was higher than in the  $\gamma$ -APS solutions. This concentration was the highest in the range 4 to 6, as recently published.<sup>22</sup> At pH values > 6, the rate of the condensation of the hydrolyzed BTSE molecules became so high that the concentration of free silanol groups was virtually zero.<sup>22</sup> Thus, BTSE films deposited from solutions in the pH range 4 pH to 6 pH could be expected to contain considerably more hydrolytically stable Fe-O-Si bonds at the interface than in the case

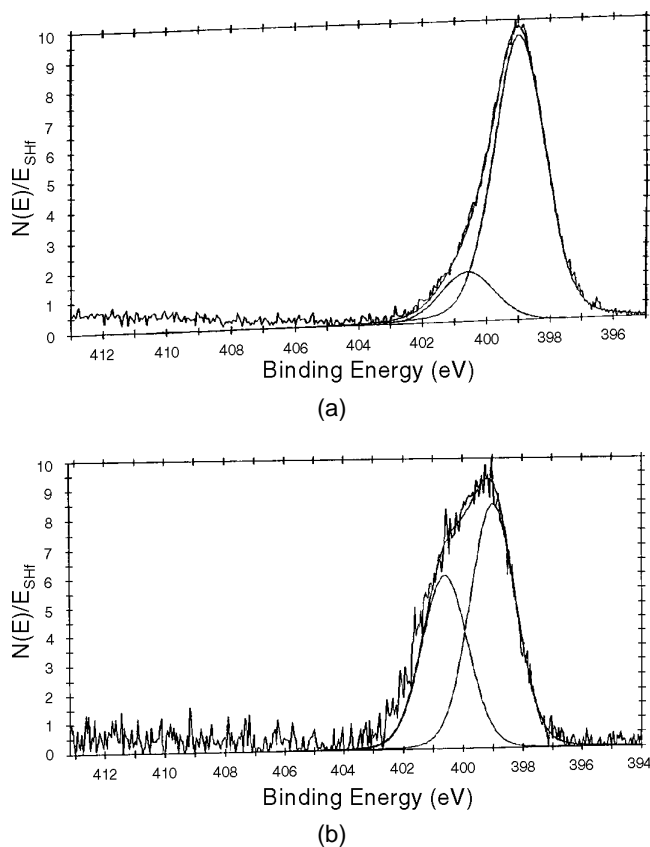


**FIGURE 8.** Deconvoluted N1s peaks for  $\gamma$ -APS films on iron: (a) before corrosion and (b) after corrosion. Concentration of the silane in solution was 4 vol%, and dipping time was 100 s. Curing was at 60°C in air for 1 h.

of  $\gamma$ -APS films and BTSE films deposited from high pH solutions. This was confirmed in a recent study where it was shown that films formed from BTSE on iron were much more resistant to rinsing the freshly deposited film with water or organic solvents than films formed by  $\gamma$ -APS alone.<sup>2</sup>

Since BTSE films contain no amino groups, the effects of protonation as a result of a lowering of the pH and subsequent  $Cl^-$  ion diffusion into the film did not occur. The only point charges in the film were negative (R-Si-O<sup>-</sup> ions), so attraction of corrosive  $Cl^-$  ions did not occur. The silanol groups were not strongly dissociated at low pH values ( $pK_a = 4$ ), so it could not be expected that the film would attract large amounts of positive ions (Na<sup>+</sup>). It also was observed that films formed from lower pH values did not trap acetate ions from the solutions, whereas films deposited from higher pH solutions contained large amounts of acetate (Figures 3 and 4). Thus, BTSE films formed at 4 pH to 6 pH had a stronger, more hydrolytically resistant interface and a lower electrical conductivity.

The hydrolysis of BTSE was an incomplete reaction. This left many Si-OC<sub>2</sub>H<sub>5</sub> groups in the BTSE

film. Some of these ester bonds were broken by the diffusing metal by the formation of Si-O-Me bonds. The ethanol molecules diffused outward. The metal atoms that were bonded in the film prevented the further dissolution of the metal outward through the film. These three factors combined were believed to be the underlying reason for the higher corrosion protection of iron by BTSE compared to  $\gamma$ -APS, as shown in Figure 1.

The steep drop in corrosion protection capability of BTSE films when deposited from a pH higher than 6 (Figure 1) was attributed to the disappearance of silanol groups in the solution. The silanol groups condensed readily at pH values > 6.<sup>22</sup> Films formed from such solutions can only bond to the iron oxide by hydrogen bonding, for instance through the oxygen atoms in the siloxane linkages or the oxygen atoms of the unhydrolyzed ethoxy ester groups. Recent studies of the kinetics of BTSE hydrolysis in water/methanol mixtures have indicated that under the conditions of hydrolysis used here, not more than 2 to 3 ester groups could be expected to be hydrolyzed to silanol groups.<sup>22</sup> Thus, the films will contain rather high concentrations of unhydrolyzed ester [-Si-(OC<sub>2</sub>H<sub>5</sub>)] groups. This already was concluded from the RA-IR spectra (Figures 4 and 5). The hydrogen bonds formed with the iron oxide surface could be expected to be sensitive to hydrolysis; hence, the corrosion protection observed with films formed from solutions of 4 pH to 6 pH was absent with the films formed from higher pHs, similar to  $\gamma$ -APS films.

In summary, this work demonstrated that amino silanes such as  $\gamma$ -APS do not function as corrosion inhibitors. However, if a bisfunctional silane ester without organofunctional groups is used, a considerable reduction of the corrosion rate in NaCl solutions can be achieved. Thus, when organofunctional silanes are used as adhesion promoters (coupling agents) for bonding metals to paints, no appreciable corrosion performance can be expected other than through improved adhesion. However, if the organofunctional coupling agent is used in combination with a nonfunctional silane, as in a two-step process, both adhesion and corrosion can be improved markedly. Recent experiments have confirmed this hypothesis for powder paint systems deposited on cold-rolled steel substrates pretreated sequentially with BTSE and  $\gamma$ -APS.<sup>21,33</sup> The process is especially effective since excellent adhesion is possible between the BTSE film formed on the metal substrate and the second layer of  $\gamma$ -APS as a result of Si-O-Si siloxane linkages.

## CONCLUSIONS

❖ Films of  $\gamma$ -APS formed on polished iron substrates of up to 0.1  $\mu$ m thickness and from solutions ranging from 4 pH to 11 pH did not have an effect on the

corrosion rate in aerated neutral NaCl solutions; these films acted as semipermeable membranes toward the diffusing species, undergoing partial dissolution simultaneously.

❖ Films of BTSE on polished iron substrates reduced the rate of iron corrosion in aerated neutral NaCl solutions by a factor of around 15 if deposited from solutions with pH 4 to 6. Films formed from higher pH values did not show any effect on the iron corrosion rate.

❖ The difference between  $\gamma$ -APS and BTSE could be explained by a mechanism based on a higher number of hydrolytically stable Fe-O-Si bonds formed by BTSE (in the pH 4 to 6 range), a lower electrical conductivity of the films and the bonding of the diffusing metal cations in the silane film. Films formed by  $\gamma$ -APS contained protonated amino groups  $-\text{NH}_3^+$  which attracted  $\text{Cl}^-$  ions into the film during the corrosion process. Further, the  $\gamma$ -APS molecules were, in part, adsorbed with the amino groups interacting with the iron oxide surface under formation of hydrolytically unstable hydrogen bonds. The diffusing metal was bonded in the BTSE film by the formation of Si-O-Me bonds from unhydrolyzed Si-OC<sub>2</sub>H<sub>5</sub> ester bonds.

❖ Silane films formed from  $\gamma$ -APS solutions and high pH BTSE solutions contained acetate ions. It was virtually impossible to obtain electrolyte-free  $\gamma$ -APS films on iron from solutions containing acetic acid or other anions.

❖ A new silane pretreatment for iron and steel surfaces was proposed consisting of sequential rinses with a nonfunctional silane such as BTSE and organofunctional silane such as  $\gamma$ -APS. This treatment was expected to improve adhesion and corrosion resistance of the metal after painting.

## ACKNOWLEDGMENTS

The authors acknowledge financial support from the U.S. Environmental Protection Agency through its Office of Research and Development under assistance agreement CR822989 to the University of Cincinnati. It has not been subjected to EPA review and, therefore, does not necessarily reflect the views of the EPA. The authors also acknowledge the assistance of R. Popat with the XPS measurements and R. Sivaraman for AFM analyses.

## REFERENCES

1. E. Plueddemann, *Silane Coupling Agents* (New York, NY: Plenum Press, 1982).
2. W.J. van Ooij, "Novel Silane-Based Metal Pretreatments to Replace Phosphates and Chromates," *Proc. Adv. Techniques for Replacing Chromium* (Johnstown, PA: Concurrent Technologies, Corp. 1996), p. 421.
3. M.A. Petrunin, A.P. Nazarov, *MPS. Sym. Proc.* 351 (1994): p. 305.
4. A. Sabata, W.J. van Ooij, H.K. Yasuda, *Surf. Interface Anal.* 20 (1993): p. 845.
5. H. Woo, P.J. Reucroft, R.J. Jacob, *J. Adhesion Sci. Technol.* 7 (1993): p. 681.
6. B. Arkles, J.R. Steinmetz, J. Zazyczny, P. Mehta, *J. Adhesion* 6 (1992): p. 193.
7. J.M. Chovelon, L.E.L. Aarch, M. Charbonnier, M. Romand, *J. Adhesion* 50 (1995): p. 43.
8. H. Ishida, "Recent Progress in the Studies of Molecular and Microstructure of Interfaces in Composites, Coatings, and Adhesive Joints," in *Adhesion Aspects of Polymeric Coatings*, ed. K.L. Mittal (New York, NY: Plenum Press, 1982).
9. F.J. Boerio, R.G. Dillingham, "Hydrothermal Stability of Titanium/Epoxy Adhesive Joints," in *Adhesive Joints: Formation, Characteristics, and Testing*, ed. K.L. Mittal (New York, NY: Plenum Press, 1984), p. 541.
10. D.E. Leyden, J. Atwater, *J. Adhesion Sci. Technol.* 5 (1991): p. 815.
11. A.M. Beccaria, M. Ghiazza, G. Poggi, *Corros. Sci.* 36 (1994): p. 1,381.
12. W.J. van Ooij, A. Sabata, *Surf. Interf. Anal.* 20 (1993): p. 475.
13. A.D. Domingue, K. Pyakis, E. Sacher, M.Di. Renzo, S. Denomme, T.H. Ellis, *Adhesion* 40 (1993): p. 151.
14. F.J. Boerio, C.H. Ho, *J. Adhesion* 21 (1987): p. 25.
15. F.J. Boerio, D.J. Ondrus, *J. Adhesion* 22 (1987): p. 1.
16. M.R. Horner, F.J. Boerio, H.M. Clearfield, *J. Adhesion Sci. Technol.* 6 (1992): p. 1.
17. P.R. Moses, M.M. Weir, J.C. Lennon, H.O. Finkler, J.R. Lenhard, R.W. Murray, *Anal. Chem.* 50 (1978): p. 576.
18. R.G. Dillingham, F.J. Boerio, *J. Adhesion* 24, (1987): p. 315.
19. W.J. van Ooij, R.A. Edwards, A. Sabata, "Metallic-Coated Steel Having a Siloxane Film Providing Temporary Corrosion Protection and Method Therefore," U.S. patent 5,292,549 to Armco Inc. (March 8, 1994).
20. W.J. van Ooij, A. Sabata, "Metal Sheet with Enhanced Corrosion Resistance having a Silane-Treated Aluminate Coating," U.S. patent 5,322,713, to Armco, Inc. (June 21, 1994).
21. B.C. Zhang, "Adsorption of Silane Films on Iron Surfaces" (Ph.D. thesis, University of Cincinnati, 1997).
22. Z. Pu, W.J. van Ooij, J.E. Mark, *J. Adhesion Sci. Technol.* 11 (1997): p. 29.
23. F.L. McCrackin, *U.S. Nat. Bur. Stand. Tech. Note* 479 (1969).
24. *Silicon Compounds — Register and Review*, 5th ed. (Bristol, PA: United Chemical Technologies, 1993).
25. P.M.A. Sherwood, "Data Analysis in XPS and AES," in *Practical Surface Analysis*, vol. 1, eds. D. Briggs, M.P. Seah (Chichester, U.K.: John Wiley and Sons, 1996).
26. R. Stefec, *Corrosion Data from Polarization Measurements* (New York, NY: Ellis Horwood, 1990).
27. F. Mansfeld, "The Polarization Resistance Technique for Measuring Corrosion Currents," in *Advances in Corrosion Science and Technology*, vol. 6, eds. M.G. Fontana, R.W. Staehle (New York, NY: Plenum Press, 1976), p. 163.
28. G. Socrates, *Infrared Characteristic Group Frequencies*, 2nd ed. (New York, NY: John Wiley and Sons, 1994).
29. W.J. van Ooij, A. Sabata, U.S. patent 5,108,793, to Armco, Inc. (April 28, 1992).
30. Infrared Spectroscopy Committee of the Chicago Society for Paint Technology, "Infrared Spectroscopy: Its Use in the Coating Industry" (Philadelphia, PA: Federation of Societies for Paint Technology, 1969).
31. F.J. Boerio, D.J. Ondrus, "Infrared and X-Ray Photoelectron Spectroscopy of Thin Silane Films on Iron and Titanium," in *Surface and Colloid Science in Computer Technology*, ed. K.L. Mittal (New York, NY: Plenum Press, 1987), p. 155.
32. B.C. Zhang, W.J. van Ooij, K.D. Connors, S.-E. Hörnström, *Organic Coatings*, ed. P.C. Lacaze (New York, NY: AIP Press, 1995), p. 305.
33. W.J. van Ooij, V. Subramanian, B.C. Zhang, U.S. patent application, Jan 9, 1997.